Wave Inversion Technology, Report No. 1, pages 77-??

Common-reflection-point stacking in laterally inhomogeneous media

Hervé Perroud, P. Hubral and G. Höcht[1]

keywords: *Imaging Stacking*

ABSTRACT

An important seismic reflection-imaging process that is widely applied in practice in an approximate form is the simulation of a zero-offset (ZO) section from a set of common-offset (CO) sections. Rather than using the familiar common-mid-point (CMP) stack (that suffers from reflection-point dispersal when the reflectors are dipping), one aims now more and more to perform an accurate common-reflection-point (CRP) stack. In the latter case, all primary CO reflections used for the simulation of a particular ZO reflection are expected to have a common reflection point. The aims of this paper are (a) to give some simple analytic formulae for these trajectories for the constant velocity case, and (b) to extend them to a CRP stacking method for 2-D laterally inhomogeneous media using only the near-surface velocity.

INTRODUCTION

CRP stacking is a widely investigated subject. Here we want to stress on a selective CRP stack, which uses only those stacking trajectories in the seismic data domain that pertain to actual reflection points. In addition to considering this CRP stacking method in 2-D constant-velocity media, we also show how to construct a CRP stack section using only the near-surface velocity. In the latter case, which can be looked upon as a brief - and hopefully new - introduction to the common-reflection-element (CRE) method of (Gelchinsky, 1988) or as a generalization of the CMP stacking method of (de Bazelaire, 1988), one obtains important wavefield attributes as part of the CRP stack. These attributes can be used to derive the complete a priori unknown 2-D laterally inhomogeneous macro-velocity model ((Hubral and Krey, 1980)).

CONSTANT-VELOCITY MEDIA

Let us consider Fig. 1, which consists of a curved dome-like subsurface reflector overlain by a constant velocity medium ($v = 2500m/s$). Let us assume that different CO profiles

[1]**email:** ghoecht@gpiwap4.physik.uni-karlsruhe.de

have been acquired, and that the CO reflection-time curve from the subsurface reflector as observed in each CO section [at the mid-point X_h between each shot S and receiver G, both separated by the constant offset $0 < 2h < 2H_{max}$] is plotted in a common $(t - x)$ domain, where t denotes time. Only two CO travel-time curves, for the offset $2h = 0m$ and $2h = 800m$, are shown in Fig. 1 in that $(t - x)$ domain. The primary reflection positions of the subsurface reflector point $R(X_r, Z_r)$ are the points $P_o(X_o, t_o)$ and $P_h(X_h, t_h)$ on the ZO and CO travel-time curves, respectively. If point P_o is ZO migrated to depth on its own, it provides the lower half-circle of radius $vt_o/2$ centered at X_o. If point P_h on the other hand is CO migrated to depth on its own, it provides the lower half-ellipse (with focal points at S and G) centered at X_h. Both the circle and the ellipse have to be tangent to the reflector at point R.

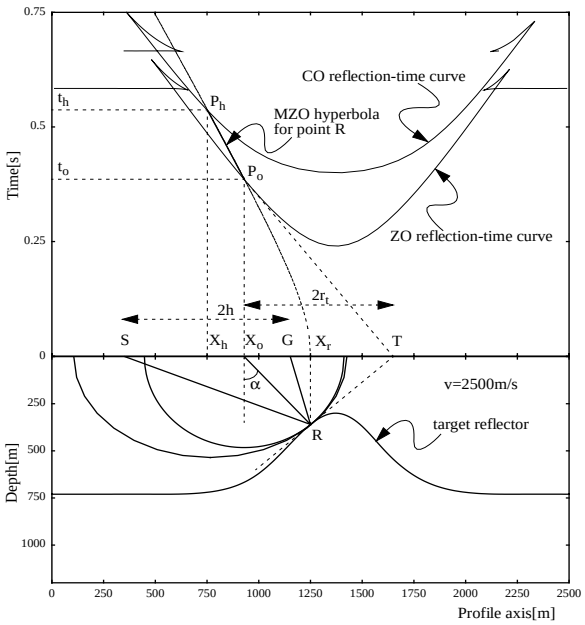

Figure 1: Lower half: Dome-like structure touched at point R by the ZO isochrone (half-circle with center at X_o) of P_o.The ray X_oRX_o denotes the ZO ray and the ray SRG the CO ray of offset $2h$. Both are specular rays and are part of the rays of the CRP configuration at X_o that illuminates point R.
Upper half: ZO reflection-time curve with point P_o and CO reflection-time curve with point P_h. Both points are connected by the MZO hyperbola (solid line) that describes the location of the CO reflections for point R as a function of the offset $2h$. The extension of the MZO hyperbola to the x-axis is dotted.

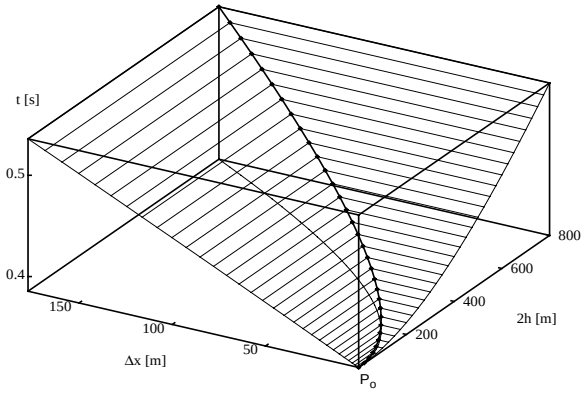

Figure 2: Isometric view of the 3-D CRP trajectory for P_o and its three 2-D projections onto the planes $t = t_o$, $h = 0$, and $\Delta x = 0$. The constant-time contours pertain to all offsets $2h$ separated by $25m$ steps.

CRP trajectories

We can now make the following interesting observation in Fig. 1 concerning all CO reflections from point R in the $(t-x)$ domain of offset $2h$: if the offset $2h$ is continuously reduced from the given value $2h$ to $2h = 0$, then point P_h moves or migrates towards P_o on what we want to call the MZO hyperbola for point R. This hyperbola is given by the following equation (1a), where v is the medium velocity and $2r_t = \overline{X_oT}$ denotes the distance between the projection X_o of point P_o onto the x-axis and point T:

$$t^2 = (4/v^2)\Delta x^2 + (8r_t/v^2 + t_o^2/2r_t)\Delta x + t_o^2 \quad (1a)$$

$$\text{with } \Delta x(h) = X - X_o = r_t\sqrt{(h/r_t)^2 + 1} - r_t \quad (1b)$$

$$\text{and } 2r_t = (v/2)(t_o/\sin\alpha) \quad (1c)$$

Point T is the point where both the tangent to the ZO reflection-time curve at P_o, and the tangent to the subsurface reflector at R, intersect with t he x-axis. The parameter α denotes the angle made by the ZO ray emerging at X_o with the vertical. The MZO hyperbola (1a) for point R is displayed in Fig. 1 as a thick line passing through points P_h and P_o.

If we consider the 3-D $(t - x - h)$ seismic data domain (here given in form of a continuous set of CO sections for $0 < 2h < 2H_{max}$), eqs. (1) define together a spatial curve in that domain. This spatial curve we call the CRP trajectory (Fig. 2) for the reflection point R of Fig. 1. The MZO hyperbola (1a) for R is therefore nothing but the projection $t(\Delta x)$ of the CRP trajectory into the $(x - t)$ plane of any CO section, e.g. for $2h = 0$. Fig. 2 also shows the projections $t(\Delta x(h))$ of eqs. (1) into the $(t - h)$ plane $\Delta x = 0$ and the projection $\Delta x(h)$ into the $(x - h)$ plane $t = t_o$.

Since each point on the $(x - h)$ plane defines one shot-receiver pair by its $x - h$ coordinates, we call the CRP configuration all shot-receiver pairs with the coordinates $(X_s = X_o + \Delta x - h, X_g = X_o + \Delta x + h)$ with Δx being given by eq. (1b) for $0 < 2h < 2H_{max}$ which illuminate point R. For this all reflected rays pass through point R.

CRP stack with selected CRP trajectories

Our purpose is now to stack only along CRP trajectories which pertain to actual reflection points. Let us for simplicity neglect the conflicting dip problem and therefore assume only one reflection point on the ZO isochrone. To identify this reflection point, we have to perform a coherency analysis along each CRP trajectory computed for each point on the ZO isochrone. The final stack for point P_o is then only performed along the CRP trajectory with the greatest coherency value. The search parameter could be the angle α of the ZO ray connecting X_o with a point on the ZO isochrone (Fig. 1), which as a result of this stack will then also be determined. We can surely admit more than one CRP trajectory to contribute to the stack value at P_o by specifying a threshold coherency value rather than selecting only the highest.

LATERALLY INHOMOGENEOUS VELOCITY

We shall now generalize the constant-velocity CRP stacking to a 2-D laterally inhomogeneous velocity medium with a constant near-surface velocity v_o. Fig. 3 shows the same target reflector as Fig. 1. It is now however overlain by two media with the constant velocities $v_o = 2500m/s$ and $v_1 = 3000m/s$.

True and auxiliary CRP experiments

In what follows, we have to clearly distinguish between concepts that have the attributes "true" and "auxiliary". They relate to either the true or auxiliary CRP experiment defined below. All graphs referring to results obtained for both experiments are shown superimposed with solid or dotted curves, respectively. In the lower half of Fig. 3, we see e.g. the true normal ray X_oRX_o. Its two-way time defines the reflection-time t_o for the ZO reflection at point P_o. Fig. 3 also shows the true CO ray SRG for a pair of points S and G that belongs to the true CRP configuration where the reflection point R is kept unchanged. If its travel-time $t = t_h$ is plotted at the midpoint X_h between the source S and the receiver G as a function of h and $\Delta x = X_h - X_o$, one obtains the true CRP trajectory of Fig. 4 with its three projections. The traces collected by the true CRP configuration are part of the true CRP experiment, where each shot is initiated at $t = 0$. The $(t - x)$ projection of the true CRP trajectory is the curve passing through points P_o and P_h in the upper half of Fig. 3.

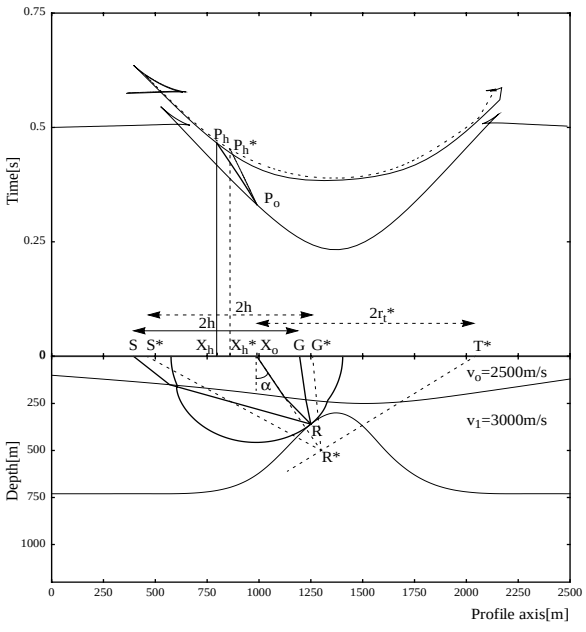

Figure 3: Lower half: Dome-like structure touched at point R by the ZO isochrone of point P_o. The ray X_oRX_o denotes the ZO ray and the ray SRG the CO ray for the true CRP experiment. Point R^* is the auxiliary reflection point of point R, i.e. the center of curvature of a wavefront originating at R and emerging at X_o.
Upper half: ZO reflection-time curve ($2h = 0m$) with point P_o and true (solid) and auxiliary (dotted) CO reflection-time curves ($2h = 800m$) with points P_h and P_h^*. Both points are connected with point P_o by the $(t - x)$ projections of the true and auxiliary 3-D CRP trajectories for point R and R^*.

The lower half of Fig. 3 also shows the so-called auxiliary reflection point R^* for the true reflection point R. Point R^* is defined as the center of curvature of the "hypothetical wavefront" that originates at point R on the true reflector and emerges at X_o. Fig. 3 also

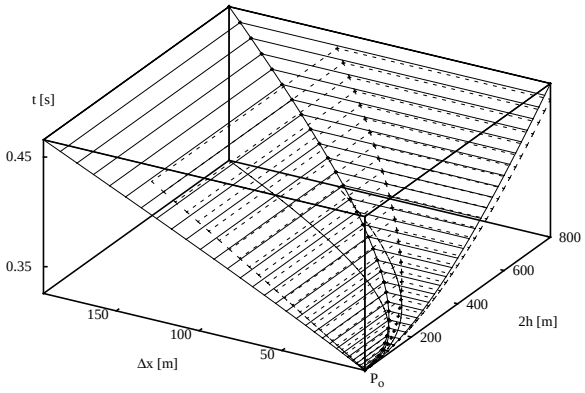

Figure 4: Superposition of two isometric views (as in Fig. 2) of the true (solid curves) and auxiliary (dotted curves) 3-D CRP trajectories and their 2-D projections for P_o.

shows the straight line from X_o to R^*. This can obviously be looked upon as the ray of an up-going hypothetical auxiliary wavefront originating at point R^* in the auxiliary velocity medium defined by the constant velocity v_o. The true and auxiliary wavefront curvatures are the same at X_o. Observe however that both hypothetical sources at R and R^* need to explode at different times if their wavefronts are expected to arrive at point X_o simultaneously. If the hypothetical source in the true velocity model at R explodes at $t = 0$, its counterpart hypothetical source (in the auxiliary velocity model v_o) at R^* should explode at $\tau = t_o/2 - r/v_o$, where r is the radius of wavefront curvature of both emerging hypothetical waves at X_o.

Let us now consider at R^* (i.e. in the auxiliary velocity model v_o) an auxiliary reflector perpendicular to $X_o R^*$. Let this be illuminated by the auxiliary CRP configuration at X_o (Fig. 3) for point R^*. This includes the shot-receiver pairs (S^*, G^*) placed at $X_s^* = X_o + \Delta x^* - h, X_g^* = X_o + \Delta x^* + h$, where

$$\begin{aligned} \Delta x^*(h) &= r_t^* \sqrt{(h/r_t^*)^2 + 1} - r_t^* \\ \text{and } 2r_t^* &= X_o T^* = r/\sin\alpha \end{aligned} \tag{2}$$

with T^* being the intersection point of the normal to the ray $X_o R^*$ at R^* with the x-axis.The auxiliary CRP experiment is now defined such that each source S^* in the auxiliary CRP configuration is initiated at $t = 2\tau$. The auxiliary CRP trajectory at $X_o = X_o^*$ for the auxiliary reflection point R^* is then given by eq. (2) and

$$(t - 2\tau)^2 = (4/v_o^2)\Delta x^{*^2} + (8r_t^*/v_o^2 + (2r/v_o)^2/2r_t^*)\Delta x^* + (2r/v_o)^2 \tag{3}$$

We observe in Fig. 4 that, since in practice we are dealing with reflection time surfaces and wavelets attached to them, the auxiliary CRP trajectory is a reasonable stacking trajectory.

CRP stack with selected CRP trajectories

To explain the essential steps of the CRP stack in unknown laterally inhomogeneous media, we reconsider Fig. 3. Since our purpose is to get a good approximation of the

travel times also for large offsets, not only the angle α but also the radii of curvature of the emerging hypothetical wavefront at X_o (originating either at R in the true model or at R^* in the auxiliary model) should coincide. Unlike in the constant velocity case where this radius of curvature equals the radius of the ZO isochrone, i.e. $r = vt_o/2$, it is unknown in laterally inhomogeneous media and therefore becomes a second search parameter. Performing e.g. a coherency analysis along the auxiliary CRP trajectories determines the stacking trajectory as well as radius of curvature r and emergence angle α for each point P_0. These are the two most important and most stable wavefield attributes that can be obtained in addition to the ZO reflection-time t_o.

CONCLUSIONS

The accuracy with which a ZO simulation in laterally inhomogeneous media can be achieved depends upon the velocity distribution above the reflectors. In fact the proposed CRP stack result may even be better than other ZO simulation stacks for an inadequately chosen velocity model. The proposed CRP stack is a selective stack, i.e. search parameters have to be found by coherency analysis, and enables us to derive the velocity model.

REFERENCES

de Bazelaire, E., 1988, Normal moveout revisited - inhomogeneous media and curved interfaces: Geophysics, **53**, no. 2, 143–157.

Gelchinsky, B., 1988, The common reflecting element (cre) method ASEG/SEG Internat. Geophys. Conf., Expl. Geophys., Extended Abstracts, 71–75.

Hubral, P., and Krey, T., 1980, Interval velocities from seismic reflection traveltime measurements *: Soc. Expl. Geophys.

Perroud, H., Hubral, P., and Höcht, G., 1996, Common-reflection-point stacking in laterally inhomogeneous media: submitted to Geophysical Prospecting.

Perroud, H., Hubral, P., Höcht, G., and de Bazelaire, E., 1997, Migrating around in circles - part III: The Leading Edge, **16**, 875–883.

PUBLICATIONS

Detailed results were published by (Perroud et al., 1996) and (Perroud et al., 1997).